



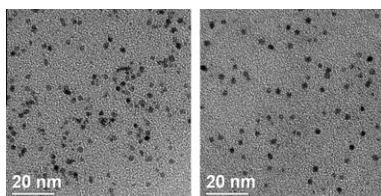
Contents

REGULAR ARTICLES

Synthesis of PVP-stabilized Pt/Ru colloidal nanoparticles by ethanol reduction and their catalytic properties for selective hydrogenation of *ortho*-chloronitrobenzene

pp 1–7

Manhong Liu*, Jin Zhang, Jinqiang Liu, William W. Yu*

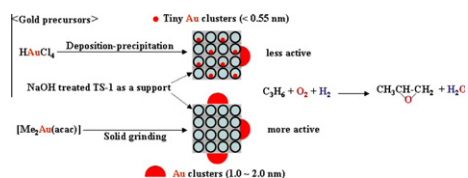


PVP-Pt/Ru colloidal nanoparticles prepared by ethanol reduction exhibit high activity and high selectivity in the selective hydrogenation of *ortho*-chloronitrobenzene to *ortho*-chloroaniline under ambient conditions. TEM photographs of PVP-Pt/Ru nanoparticles: 4Pt/1Ru (left), 2Pt/1Ru (right).

Propene epoxidation with O₂ and H₂: Identification of the most active gold clusters

pp 8–15

Jiahui Huang, Enrique Lima*, Tomoki Akita, Ariel Guzmán, Caixia Qi, Takashi Takei, Masatake Haruta*

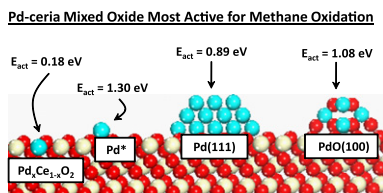


In propene epoxidation with O₂ and H₂, Au clusters (1.0–2.0 nm) on exterior surfaces of TS-1 treated with NaOH were more active than tiny Au clusters (<0.55 nm) inside micropores.

Methane oxidation on Pd–Ceria: A DFT study of the mechanism over Pd_xCe_{1–x}O₂, Pd, and PdO

pp 16–25

Adam D. Mayernick, Michael J. Janik*

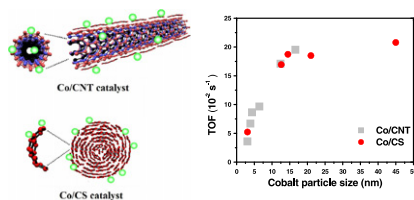


The methane activation barrier over the Pd_xCe_{1–x}O₂(1 1 1) surface is lower than that over CeO₂(1 1 1), Pd(1 1 1), or PdO(1 0 0). Methane activation is rate limiting in all cases; thus, the low barrier over Pd_xCe_{1–x}O₂ evidences the unique hydrocarbon oxidation activity of Pd/ceria mixed oxides.

Correlating the preparation and performance of cobalt catalysts supported on carbon nanotubes and carbon spheres in the Fischer–Tropsch synthesis

pp 26–40

Haifeng Xiong, Myriam A.M. Motchelaho, Mahluli Moyo, Linda L. Jewell, Neil J. Coville*

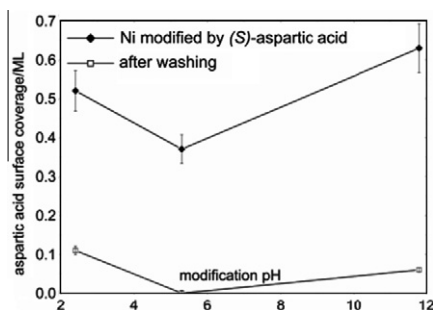


Carbon nanotubes (CNTs) and carbon spheres (CSs) were used to load cobalt with different cobalt particle sizes for use in FTS. The similarities and differences between Co/CNT and Co/CS were investigated.

XPS studies of the effects of modification pH on the interaction of methylacetoacetate with (S)-aspartic acid-modified Ni surfaces

pp 41–49

Karen E. Wilson, Christopher J. Baddeley*

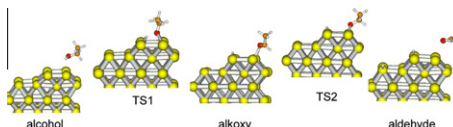


Ni catalysts modified by (S)-aspartic acid exhibit a sharp maximum in enantioselectivity following modification at pH 5.0 and 300 K. XPS shows that under these conditions the coverage of aspartate is vanishingly small implying that enantioselectivity, in this case, may be derived from chiral metal sites created by the corrosive leaching of Ni by aspartic acid.

Mechanism of selective alcohol oxidation to aldehydes on gold catalysts: Influence of surface roughness on reactivity

pp 50–58

Mercedes Boronat, Avelino Corma*, Francesc Illas, Juan Radilla, Tania Ródenas, María J. Sabater

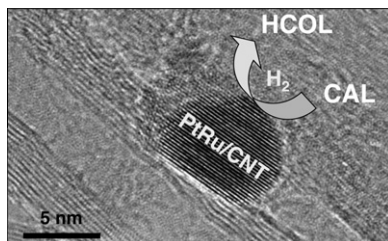


A complete DFT study of the mechanism of selective alcohol oxidation on a series of Au catalyst models suggests that the activity of Au sites inversely correlates with their coordination number. This hypothesis is experimentally confirmed by a kinetic study of benzyl alcohol oxidation on a series of Au/MgO catalyst differing in Au particle diameter and therefore in concentration and distribution of low coordinated Au sites.

Influence of particles alloying on the performances of Pt–Ru/CNT catalysts for selective hydrogenation

pp 59–70

Jacques Teddy, Andrea Falqui, Anna Corrias, Daniela Carta, Pierre Lecante, Iann Gerber, Philippe Serp*

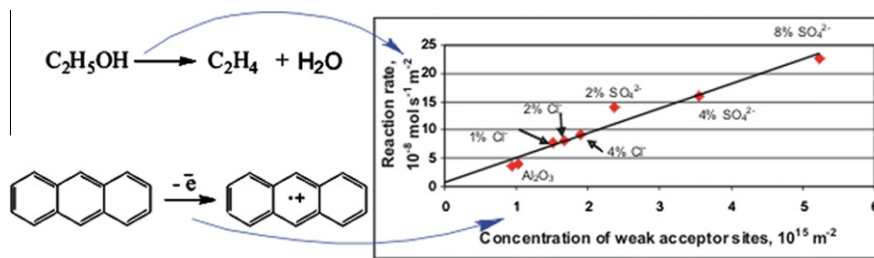


Very active and selective Pt–Ru/CNT catalysts have been prepared for the selective hydrogenation of cinnamaldehyde into cinnamyl alcohol. Characterization using HRTEM, WAXS and EXAFS was indicative of the influence of particles alloying on the selectivity of these systems.

Characterization of the active sites on the surface of Al_2O_3 ethanol dehydration catalysts by EPR using spin probes

pp 71–77

Ruslan A. Zotov, Viktor V. Molchanov, Alexander M. Volodin, Alexander F. Bedilo*

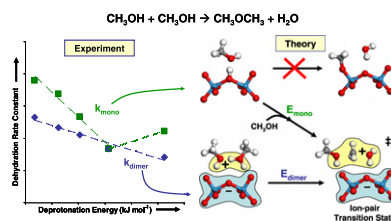


An excellent correlation between the activity of anion-doped alumina catalysts in ethanol dehydration and the concentration of weak acceptor sites capable of ionizing anthracene has been observed.

Catalytic consequences of acid strength in the conversion of methanol to dimethyl ether

pp 78–93

Robert T. Carr, Matthew Neurock, Enrique Iglesia*

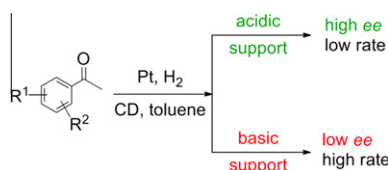


Dimethyl ether synthesis on solid acids occurs via direct reactions of two co-adsorbed CH_3OH molecules because methyl cations at transition states are effectively solvated by H_2O and CH_3OH molecules. On acids, activation barriers and their sensitivity to acid strength depend on differences in charge distribution and density in adsorbed reactants and their respective transition states.

Hydrogenation of acetophenone derivatives: Tuning the enantioselectivity via the metal–support interaction

pp 94–101

Fatos Hoxha, Erik Schmidt, Tamas Mallat, Bjoern Schimmoeller, Sotiris E. Pratsinis, Alfons Baiker*

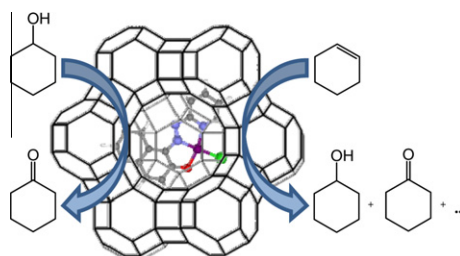


The acid–base properties of the support interaction control the rate and the selectivity of the hydrogenation of acetophenone derivatives to alcohol, and also the adsorption mode and the rate of degradation of cinchonidine (CD) on the Pt surface.

Catalytic behavior of 1-(2-pyridylazo)-2-naphthol transition metal complexes encapsulated in Y zeolite

pp 102–110

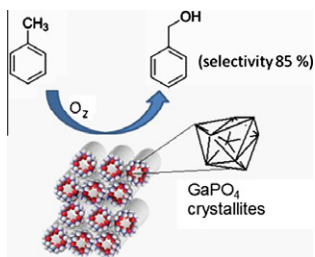
I. Kuźniarska-Biernacka, K. Biernacki, A.L. Magalhães, A.M. Fonseca, I.C. Neves*



Zeolite-supported transition metal complexes with PAN ligand have been prepared by flexible ligand method; these guest–host catalysts are more active in cyclohexanol oxidation than cyclohexene. Heterogenized zinc(II) complex is the best catalyst among the complexes analyzed; in addition, it was shown that it possesses distinct geometrical features.

High-surface thermally stable mesoporous gallium phosphates constituted by nanoparticles as primary building blocks pp 111–122

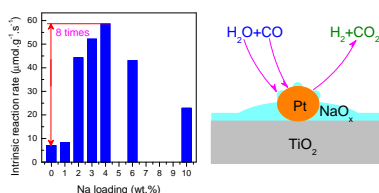
Vasile I. Parvulescu*, Viorica Parvulescu, Dragos Ciuparu, Christopher Hardacre, Hermenegildo Garcia*



Mesoporous gallium phosphates synthesized by hydrolysis of gallium alkoxide in the presence of PCl_3 assisted by surfactants form robust structures exhibiting the potential of the aerobic oxidation of toluene.

Structural effects of Na promotion for high water gas shift activity on Pt–Na/TiO₂ pp 123–132

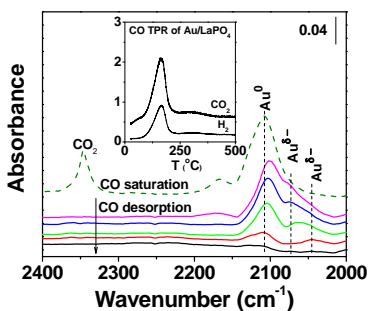
Xinli Zhu, Min Shen, Lance L. Lobban, Richard G. Mallinson*



Intrinsic reaction rate and turnover frequency of water gas shift reaction at 300 °C are improved 8 and 11 times, respectively, for Pt/TiO₂ catalyst with optimal Na loading (Na/Pt = 34). Characterizations reveal the strong metal–promoter interactions between Pt and NaO_x are responsible for the significant improvement in activity and stability.

CO oxidation on phosphate-supported Au catalysts: Effect of support reducibility on surface reactions pp 133–142

Meijun Li, Zili Wu, S.H. Overbury*

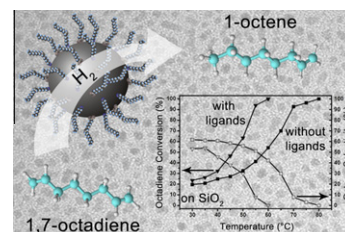


Unexpectedly, CO interacts rapidly with Au/LaPO₄ to evolve CO₂ even though the LaPO₄ is non-reducible. H₂ evolves with CO₂ during CO-TPR of Au/LaPO₄ (but not for Au/FePO₄) so surface hydroxyls react to oxidize CO, catalyzed by the Au, a pathway competing with direct CO oxidation.

Heterogeneous catalysis with supported platinum colloids: A systematic study of the interplay between support and functional ligands pp 143–152

X. Wang, P. Sonström, D. Arndt, J. Stöver, V. Zielasek, H. Borchert, K. Thiel, K. Al-Shamery, M. Bäumer*

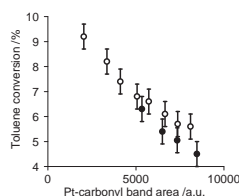
The catalytic properties of identical colloiddally synthesized ligand-free and ligand-capped Pt nanoparticles supported on different oxides (γ -Al₂O₃, MgO and SiO₂) were studied under oxidative as well as reductive conditions. In the case of the ligand-free nanoparticles, surface oxidation was observed after deposition in dependence of the support's Brønsted acidity. In contrast, the presence of ligands effectively prevented such a metal support interaction, in turn leading to superior hydrogenation activity at low temperatures (<100 °C). At higher temperatures (~200 °C), spillover of ligands from the nanoparticles to the support led to a decrease of the ligand coverage, resulting in higher CO oxidation activities especially for Lewis acidic supports. The study reveals that organic ligands of colloiddally prepared particles are not necessarily detrimental for catalytic activity. In some cases, they can exert a protective function, in other cases spillover onto the support minimizes negative effects resulting from blocking of catalytic sites.



Correlation between deactivation and Pt-carbonyl formation during toluene hydrogenation using a H₂/CO₂ mixture

pp 153–161

Aqeel Ahmad Taimoor, Isabelle Pitault*, Frédéric C. Meunier*

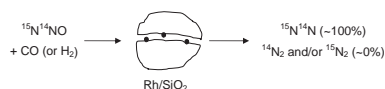


The loss of toluene hydrogenation activity is due to the formation of Pt-carbonyl species when using a CO₂-containing feed.

NOTES**The reduction of ¹⁵N¹⁴NO by CO and by H₂ over Rh/SiO₂: A test of a mechanistic proposal**

pp 162–166

Noel W. Cant*, Dean C. Chambers, Irene O.Y. Liu

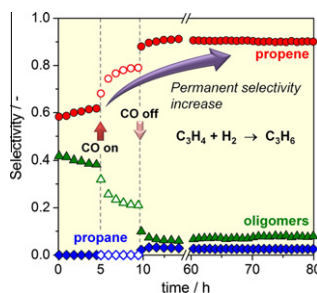


The reduction of ¹⁵N¹⁴NO by carbon monoxide, and also by hydrogen, over a Rh/SiO₂ catalyst yields ¹⁵N¹⁴N as the exclusive nitrogen-containing product. The result rules out a suggestion in the literature that the reduction using carbon monoxide proceeds through cleavage of the nitrogen–nitrogen bond.

Permanent alkene selectivity enhancement in copper-catalyzed propyne hydrogenation by temporary CO supply

pp 167–172

Blaise Bridier, Miguel A.G. Hevia, Nuria López, Javier Pérez-Ramírez*



Temporary addition of CO during propyne hydrogenation on a copper catalyst permanently boosts the propene selectivity by inducing a smaller ensemble that cuts down the oligomerization path.